Inorg. Chem. **2006**, *45*, 3718–3725

Pressure Effect on Bulk Weak Ferromagnets: (BDH-TTP)[M(isoq)$_2$(NCS)$_4$] (M = Cr^{III}, Fe^{III}; isoq = Isoquinoline)

Satoshi Kudo,[†] Akira Miyazaki,*[,†] Toshiaki Enoki,*[,†] Stéphane Golhen,[‡] Lahcène Ouahab,[‡] Takashi Toita,[§] and Jun-ichi Yamada[§]

Department of Chemistry, Tokyo Institute of Technology, 2-12-1 O-okayama, Meguro-ku, Tokyo 152-8551, Japan, Sciences Chimiques de Rennes, Equipe Organométalliques et Matériaux Moléculaires, UMR CNRS 6226, Université de Rennes 1, 35042 Rennes Cedex, France, and Department of Material Science, University of Hyogo, 3-2-1 Kouto, Kamigori, Hyogo 678-1297, Japan

Received October 29, 2005

The pressure dependence of the magnetic properties of weak ferromagnets (BDH-TTP)[M(isoq)$_2$(NCS)$_4$] [BDH-TTP = 2,5-bis(1′,3′-dithiolan-2′-ylidene)-1,3,4,6-tetrathiapentalene; M = Cr, Fe; isoq = isoquinoline] is discussed. These salts form two-dimensional magnetic sheets, where ferrimagnetic chains of donor cation radical ($S = {}^1/_2$) and anion [$S = {}^3/_2$ (Cr), ${}^5/_2$ (Fe)] are antiferromagnetically connected by weak donor–donor and anion–anion interchain S···S contacts. Under ambient pressure, both the Cr and Fe salts undergo a weak ferromagnetic transition at $T_c = 7.6$ K, below which a spontaneous magnetization emerges along the direction perpendicular to the sheets. The application of the pressure elevates the transition temperatures up to 16.6 and 11.6 K at 9 kbar for M = Cr and Fe, respectively. As the pressure increases, the remanent magnetization M_r decreases, whose pressure dependence for the Cr salt is larger than that for the Fe salt. This difference indicates that the spin-canting angle of the Cr salt is reduced because of the increase of antiferromagnetic interaction by applied pressure, in contrast to the Fe salt, where single-ion anisotropy contributes less. The quantitative analysis of the magnetization curves of the Cr salt using the mean-field approximation reveals that the intermolecular exchange interaction increases as the pressure increases, among which the interchain anion–anion interaction has the highest pressure sensitivity. This result is consistent with the temperature dependence of the crystal structure showing that the thermal contraction in the distances of interchain anion–anion S···S contacts is the most remarkable in intrachain S···S contacts. The large pressure dependence of the transition temperature of these salts is therefore explained as a result of the fact that the interchain interactions, the anion–anion interaction in particular, are strengthened by applied pressure.

Introduction

Charge-transfer salts composed of organic donors and magnetic transition-metal complexes give $\pi-$d composite magnetic systems, in which an intermolecular exchange interaction between donor π-electron spin and anion d-electron spin ($\pi-$d interaction) plays an important role.[1−11] When the π electrons on the donor layer have localized character, the interplay of two kinds of spins in donor and acceptor with different spin quantum numbers and the magnetic anisotropies brings about a large variety of

* To whom correspondence should be addressed. E-mail: miyazaki@chem.titech.ac.jp (A.M.), tenoki@chem.titech.ac.jp (T.E.).
[†] Tokyo Institute of Technology.
[‡] Université de Rennes 1.
[§] University of Hyogo.

(1) Miyazaki, A.; Enomoto, K.; Okabe, K.; Yamazaki, H.; Nishijo, J.; Enoki, T.; Ogura, E.; Ugawa, K.; Kuwatani, Y.; Iyoda, M. *J. Solid State Chem.* **2002**, *168*, 547−562.
(2) Miyazaki, A.; Okabe, K.; Enomoto, K.; Nishijo, J.; Enoki, T.; Setifi, F.; Golhen, S.; Ouahab, L.; Toita, T.; Yamada, J. *Polyhedron* **2003**, *22*, 2227−2234.
(3) Kobayashi, H.; Kobayashi, A.; Cassoux, P. *Chem. Soc. Rev.* **2000**, *29*, 325−333.
(4) Uji, S.; Shinagawa, H.; Terashima, T.; Yakabe, T.; Terai, Y.; Tokumoto, M.; Kobayashi, A.; Tanaka, H.; Kobayashi, H. *Nature* **2001**, *410*, 908−910.
(5) Hanasaki, N.; Tajima, H.; Matsuda, M.; Naito, T.; Inabe, T. *Phys. Rev. B* **2000**, *62*, 5839−5842.
(6) Nishijo, J.; Ogura, E.; Yamaura, J.; Miyazaki, A.; Enoki, T.; Takano, T.; Kuwatani, Y.; Iyoda, M. *Solid State Commun.* **2000**, *116*, 661−664.
(7) Enomoto, K.; Miyazaki, A.; Enoki, T. *Bull. Chem. Soc. Jpn.* **2001**, *74*, 459−470.
(8) Coronado, E.; Galán-Mascarós, J. R.; Gomez-García, C. J.; Laukhin, V. *Nature* **2000**, *408*, 447−449.

10.1021/ic0518778 CCC: $33.50
Published on Web 03/28/2006

Chart 1

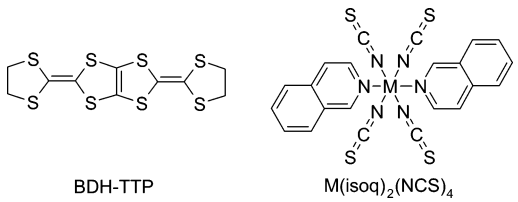

magnetic structures, in which ferrimagnetism typically appears. Among these $\pi-$d composite molecular magnets, (BDH-TTP)[M(isoq)$_2$(NCS)$_4$] (BDH-TTP = 2,5-bis(1′,3′-dithiolan-2′-ylidene)-1,3,4,6-tetrathiapentalene; M = Cr, Fe; isoq = isoquinoline; Chart 1) is most interesting because of the presence of weak ferromagnetism based on a competition between the magnetic anisotropies and the antiferromagnetic (AF) interaction between the π and d counterparts. Indeed, these salts show a bulk weak ferromagnetism at 7.6 K for both M = Cr and Fe.[2,12,13] In the crystals of these complexes, transition-metal complex anions $[M^{III}(isoq)_2(NCS)_4]^-$ [$S = {}^3/_2$ (Cr), ${}^5/_2$ (Fe)] having π-electron-based ligands (isoquinoline and NCS coordinated at the axial and equatorial positions, respectively) interact with the cation radical of BDH-TTP ($S = {}^1/_2$)[14,15] with close intermolecular S···S contacts to form ferrimagnetic chains parallel to the *c* axis. These chains are then antiferromagnetically coupled with each other by other S···S contacts along the *a* axis between anions and between donors (Figure 1). The origin of the weak ferromagnetism is characterized as a spin canting because of the noncollinear alignment of the neighboring [M(isoq)$_2$(NCS)$_4$] anions belonging to the adjacent ferrimagnetic chains, where the anisotropy axes are oriented to the isoq−M−isoq direction of the each anion, with the mutual angle being 34°. Because of this geometry, single-ion anisotropy and/or antisymmetric Dzyaloshinsky−Moriya (D−M) interaction[16−18] between the anions leads to their noncollinear spin alignment. In other words, the spin structures of these salts are stabilized by a subtle competition between the exchange interaction and magnetic anisotropy. This situation is similar to the case of rare-earth orthoferrites $RFeO_3$,[19−22] in which an AF interaction between the axially distorted FeO_6 octahedra with noncollinear alignment produces a spin-canted weak ferromagnetism. The origin of the spin canting is characterized as the D−M interaction between Fe^{3+} spins

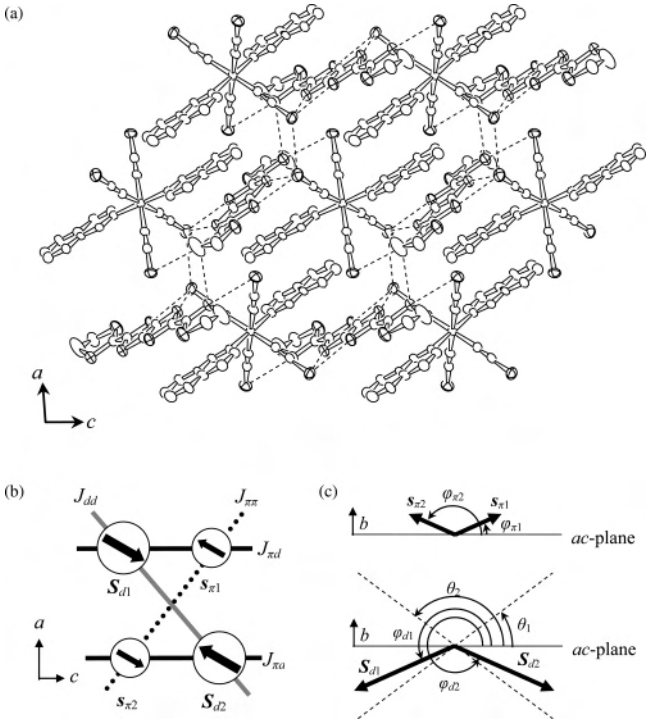

Figure 1. (a) Crystal structure of (BDH-TTP)[M(isoq)$_2$(NCS)$_4$] (M = Cr, Fe) at 120 K after ref 12. The dashed lines indicate intermolecular S···S contacts. (b) Schematic spin structure model containing two localized π spins (short arrows labeled π_1 and π_2) and two d spins (long arrows labeled d_1 and d_2). $J_{\pi\pi}$, $J_{\pi d}$, and J_{dd} represent donor−donor, donor−anion, and anion−anion exchange interactions, respectively. (c) Orientations of the π (top) and d (bottom) spins tilted from the *ac* plane. φ_{π_1}, φ_{π_2}, φ_{d_1}, and φ_{d_2} represent the spin-canting angles of π_1, π_2, d_1, and d_2 from the *ac* plane. Dashed lines are anisotropy axes of the d spins determined by isoq−M−isoq axes, and θ_1 and θ_2 are their canting angles from the *ac* plane.

rather than single-ion anisotropy of the axially distorted Fe^{3+} octahedra, by static torque measurements.[20,21]

Because the molecular magnets such as the titled compounds have soft lattices compared to inorganic magnets, it is expected that even a slight external pressure can easily modify the spin structure. Namely, the application of pressure, which can change the molecular arrangement in the molecular crystals owing to their flexibility and softness, is expected to vary this competition and thus the spin structure. Actually, it has been reported that simple molecule-based canted antiferromagnets such as 1,3,5-triphenyl-6-oxoverdazyl (TOV)[23,24] and dithiadiazolyl radical *p*-NC·C_6F_4·CNSSN[25,26] show large pressure dependences of their magnetic transition temperatures (TOV, $T_c = 5.0$ K at $p =$ 1 bar, 10.5 K at 10 kbar;[24] *p*-NC·C_6F_4·CNSSN, $T_c = 35.5$ K at 1 bar, 64.5 K at 16.5 kbar[26]). In these materials, the origin of the spin canting is ascribed to the D−M interaction (because for $S = {}^1/_2$, there is no single-ion anisotropy), and the enhancement of the intermolecular exchange interaction

(9) Ouahab, L.; Enoki, T. *Eur. J. Inorg. Chem.* **2004**, 933−941.
(10) Coronado, E.; Day, P. *Chem. Rev.* **2004**, 5419−5448.
(11) Enoki, T.; Miyazaki, A. *Chem. Rev.* **2004**, 5449−5477.
(12) Setifi, F.; Golhen, S.; Ouahab, L.; Miyazaki, A.; Okabe, K.; Enoki, T.; Toita, T.; Yamada, J. *Inorg. Chem.* **2002**, *41*, 3786−3790.
(13) Miyazaki, A.; Okabe, K.; Enoki, T.; Setifi, F.; Golhen, S.; Ouahab, L.; Toita, T.; Yamada, J. *Synth. Met.* **2003**, *137*, 1195−1196.
(14) Yamada, J.; Watanabe, M.; Anzai, H.; Nishikawa, H.; Ikemoto, I.; Kikuchi, K. *Angew. Chem., Int. Ed.* **1999**, *38*, 810−813;
(15) Yamada, J.; Watanabe, M.; Akutsu, H.; Nakatsuji, S.; Nishikawa, H.; Ikemoto, I.; Kikuchi, K. *J. Am. Chem. Soc.* **2001**, *123*, 4174−4180.
(16) Dzyaloshinsky, I. *J. Phys. Chem. Solids* **1958**, *4*, 241−255.
(17) Moriya, T. *Phys. Rev.* **1960**, *117*, 635−647.
(18) Moriya, T. *Phys. Rev.* **1960**, *120*, 91−98.
(19) White, R. L. *J. Appl. Phys.* **1969**, *40*, 1061−1069.
(20) Treves, D. *Phys. Rev.* **1962**, *125*, 1843−1853.
(21) Gorodetsky, G.; Treves, D. *Phys. Rev.* **1964**, *135*, A97−A101.
(22) Eibschütz, M.; Shtrikman, S.; Treves, D. *Phys. Rev.* **1967**, *156*, 562−577.
(23) Mito, M.; Nakano, H.; Kawae, T.; Hitaka, M.; Takagi, S.; Deguchi, H.; Suzuki, K.; Mukai, K.; Takeda, K. *J. Phys. Soc. Jpn.* **1997**, *66*, 2147−2156.
(24) Mito, M.; Hitaka, M.; Kawae, T.; Takeda, K.; Suzuki, K.; Mukai, K. *Mol. Cryst. Liq. Cryst.* **1999**, *334*, 369−378.
(25) Banister, A. J.; Bricklebank, N.; Lavender, I.; Rawson, J. M.; Gregory, C. I.; Tanner, B. K.; Clegg, W.; Elsegood, M. R. J.; Palacio, F. *Angew. Chem., Int. Ed. Engl.* **1996**, *35*, 2533−2535.
(26) Mito, M.; Kawae, T.; Takeda, K.; Takagi, S.; Matsushita, Y.; Deguchi, H.; Rawson, J. M.; Palacio, F. *Polyhedron* **2001**, *20*, 1509−1512.

Table 1. Crystallographic Data of (BDH-TTP)[M(isoq)$_2$(NCS)$_4$]

	temp/K		
	293	120[a]	18
	M = Cr (Chemical Formula = $C_{32}H_{22}CrN_6S_{12}$, fw = 927.28)		
cryst syst	monoclinic	monoclinic	monoclinic
space group	*C*2/*c*	*C*2/*c*	*C*2/*c*
a/Å	16.1944(11)	16.1363(9)	16.0921(7)
b/Å	19.2325(12)	19.0874(12)	19.0138(9)
c/Å	12.6558(10)	12.5075(6)	12.4404(6)
β/deg	95.687(3)	95.237(2)	94.1315(19)
V/Å^3	3922.4(5)	3833.3(5)	3796.5(3)
Z	4	4	4
no. of obsd reflns [$I > 2\sigma(I)$]	1993	2844	2761
R1[b]	0.054	0.052	0.037
wR2[b]	0.134	0.119	0.100
	M = Fe (Chemical Formula = $C_{32}H_{22}FeN_6S_{12}$, fw = 931.13)		
cryst syst	monoclinic	monoclinic	monoclinic
space group	*C*2/*c*	*C*2/*c*	*C*2/*c*
a/Å	16.2691(9)	16.1938(8)	16.0921(7)
b/Å	19.2402(11)	19.1117(11)	19.0138(9)
c/Å	12.6693(8)	12.5100(10)	12.4404(6)
β/deg	95.237(2)	94.265(3)	93.7432(14)
V/Å^3	3949.2(4)	3861.0(4)	3824.5(2)
Z	4	4	4
no. of obsd reflns [$I > 2\sigma(I)$]	2632	2967	3192
R1[b]	0.051	0.048	0.038
wR2[b]	0.123	0.113	0.088

[a] After ref 12. [b] $R1 = \sum(||F_o| - |F_c||)/\sum|F_o|$. $wR2 = [\sum w(|F_o|^2 - |F_c|^2)^2/\sum w(|F_o|^2)^2]^{1/2}$.

increases the transition temperature. Therefore, it is also expected that the application of the pressure allows us to understand the magnetism of (BDH-TTP)[M(isoq)$_2$(NCS)$_4$] comprehensively and systematically. In this paper, we discuss the magnetic properties of (BDH-TTP)[M(isoq)$_2$(NCS)$_4$] under pressure and evaluate the pressure dependence of the exchange interaction. We also report the temperature dependence of the crystal structure of these salts, to discuss the origin of the pressure effect of the intermolecular exchange interaction between the localized moments.

Experimental Section

Single-crystalline samples of (BDH-TTP)[M(isoq)$_2$(NCS)$_4$] (M = Cr, Fe) were prepared as previously reported.[3] Magnetic susceptibility and magnetization were measured using a Quantum-Design MPMS-5 SQUID magnetometer up to a field of 5.5 T in the temperature range 2−300 K. The hydrostatic pressure was applied to the sample using a Be−Cu clamp cell (ElectroLAB Co. Ltd.) up to 10 kbar (=1 GPa) with Daphne 7373 oil as a pressure medium. The applied pressure at low temperatures was calibrated by the pressure dependence of the superconducting transition temperature of Sn[27] enclosed in the clamp cell as a reference. For the Cr salt, single platelike crystals (ca. 0.2 mg) were aligned and attached with Apiezon N grease on the flat end of a quartz rod that is inserted in the pressure cell. For the Fe crystals, nonoriented microcrystals (1.0 mg) were used for the measurements because of the less-developed crystal habits of the available samples.

The crystal structure of the Cr and Fe salts were determined by X-ray crystallography. Single crystals were mounted on a Nonius Kappa CCD diffractometer (CDFIX, Université de Rennes 1, Rennes, France) equipped with a CCD camera and graphite-monochromated Mo Kα radiation (λ = 0.710 73 Å). The sample temperature was regulated with an Oxford Diffraction Cryojet and a Helijet temperature controller for the measurements at T = 120 and 18 K, respectively. The effective absorption correction was made for the integrated intensity data (*SCALEPACK*). Structures were solved with direct methods and refined with a full-matrix least-squares method on F^2 using *SHELX-97* programs.[28] Crystallographic data are summarized in Table 1. Full atomic coordinates, bond lengths, and bond angles are deposited as Supporting Information.

Results

Parts a and b of Figure 2 show the temperature dependence of the remanent magnetization $M_r(T,p)$ for the Cr and Fe salts, respectively, under different pressures after an external field of 1 T was removed at 2 K. The long-range magnetic transition temperature T_c, defined as the temperature where M_r disappears, increases as the pressure increases for both salts. This result suggests that the applied pressure strengthens the AF interaction, although the trends in their pressure dependence are different between the two salts, as shown in Figure 2c. The pressure dependence of T_c is expressed as a linear function of p as

$$T_c(p) = T_c(p_0)\,[1 + \gamma p] \qquad (1)$$

where p_0 is the ambient pressure and the coefficient γ is estimated as 0.132 and 0.058 kbar^{-1} for M = Cr and Fe, respectively. These coefficients are comparable to molecule-based bulk antiferromagnets such as 2,2,6,6-tetramethyl-4-piperidinol-1-oxyl (=TANOL, $T_N(p_0)$ = 0.49 K, γ = 0.15 kbar^{-1})[29] or canted antiferromagnets TOV (0.086 kbar^{-1})[24]

(27) Uwatoko, Y.; Hotta, T.; Matsumoto, E.; Mori, H.; Ohki, T.; Sarrao, J. L.; Thompson, J. D.; Mori, N.; Oomi, G. *Rev. High-Pressure Sci. Technol*. **1998**, *7*, 1508−1510.

(28) Sheldrick, G. M. *SHELX-97, Program for the Refinement of Crystal Structures*; University of Göttingen: Göttingen, Germany, 1997.

(29) Takeda, K.; Uryû, N.; Inoue, M.; Yamauchi, J. *J. Phys. Soc. Jpn.* **1987**, *56*, 736−741.

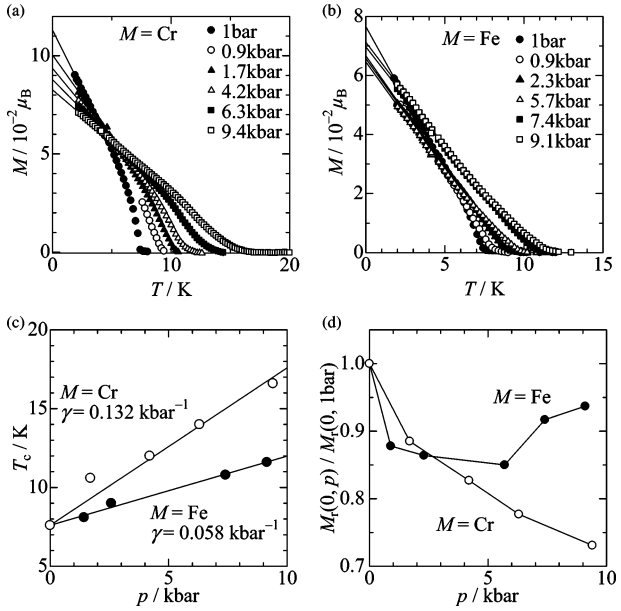

Figure 2. (a) Temperature dependence of remanent magnetization $M_r(T,p)$ for BDH-TTP[Cr(isoq)$_2$(NCS)$_4$] (single-crystalline samples; M_r parallel to *b*) under different pressures. Solid lines are linear fitting curves of $M_r(T,p)$ for $T < T_c/2$ to obtain $M_r(0,p)$ (see the text). (b) Temperature dependence of M_r for BDH-TTP[Fe(isoq)$_2$(NCS)$_4$] (nonoriented microcrystalline samples) under different pressures. Solid lines are similar to those in part a . (c) Pressure dependence of the magnetic transition temperature T_c for the Cr (open circles) and Fe (filled circles) salts. Solid lines are the linear fitting with $T_c(p) = T_c(p_0)\ [1 + \gamma p]$. (d) Pressure dependence of the remanent magnetization $M_r(0,p)$ for the Cr (open circles) and Fe (filled circles) salts normalized with $M_r(0,p) = 1$ bar. Solid lines are guides for the eyes.

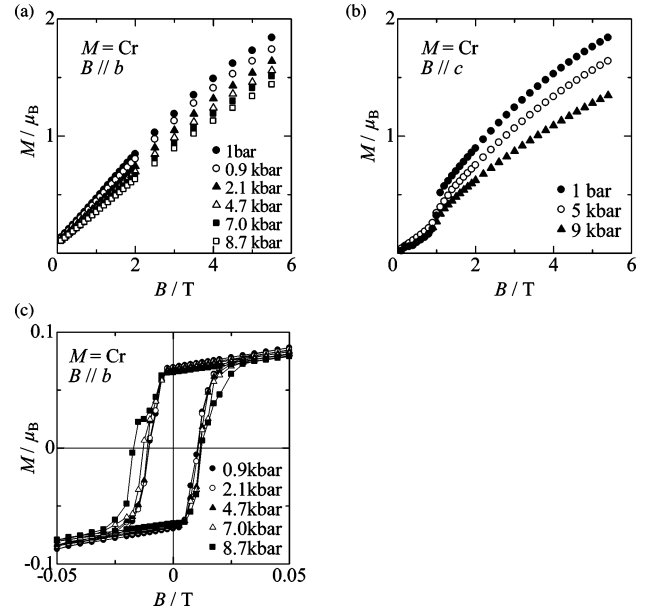

Figure 3. (a and b) Magnetization curves of the Cr salt measured at $T = 2$ K under different pressures [(a) *B* parallel to *b*; (b) *B* parallel to *c*]. (c) Hysteresis loops of the Cr salt at $T = 2$ K under different pressures.

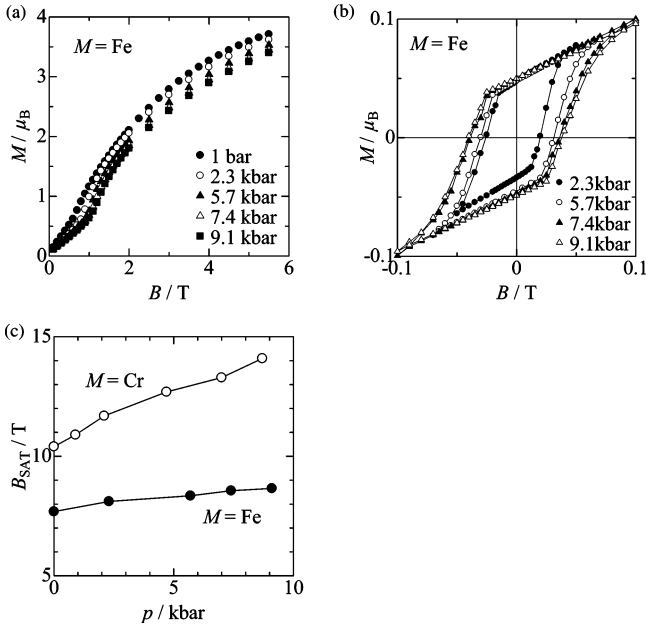

Figure 4. (a) Magnetization curves of the Fe salt measured at $T = 2$ K (nonoriented microcrystalline samples). (b) Hysteresis loops of the Fe salt at $T = 2$ K under different pressures. (c) Pressure dependence of the saturation field B_{SAT} for the Cr (open circles) and Fe (filled circles) salts. Solid lines are guides for the eyes.

and are significantly larger than inorganic antiferromagnets such as $CoCl_2 \cdot 6H_2O$ (0.038 kbar^{-1}).[30] Interestingly, at 9.4 kbar T_N of the Cr salt reaches 16.6 K, which is twice the value at ambient pressure (7.6 K) without showing a trend of saturation. Figure 2d shows the pressure dependence of $M_r(0,p)$ defined by a linear extrapolation of $M_r(T,p)$ to $T = 0$ K using the data in the temperature range $T < T_c/2$ [below this temperature, $M_r(T,p)$ curves can be regarded as a linear function of the temperature]. For the Cr salt, $M_r(0,p)$ monotonically decreases as the pressure increases, with the decrement in $M_r(0,p)$ being 27% at 9.4 kbar. This trend is confirmed by the presence of a clear intersection of the $M_r(T,p)$ plots at $T \sim 4.5$ K. On the other hand, $M_r(0,p)$ for the Fe salt has a smaller pressure dependence, with a decrement of, at most, 15% at 5.7 kbar. The nonuniform pressure dependence of $M_r(0,p)$ for the Fe salt might come from an extrinsic effect, such as inhomogeneity of the applied pressure to the nonoriented samples.

Parts a and b of Figure 3 show the magnetization curves of the Cr salt measured at $T = 2$ K with the external field parallel to the *b* and *c* axes, respectively. For both directions of the fields, the magnetization decreases as the pressure increases. When the field is applied parallel to the *b* axis, a nonvanishing magnetization appears at $B = 0$, corresponding to the values of $M_r(2,p)$ in Figure 2a. When the field is applied parallel to the *c* axis, the spin−flop transition is observed around 1 T, as evidenced by a steep increase appearing in the magnetization curves in Figure 3b. This spin−flop field B_{SF} is almost independent of the pressure. For the randomly oriented crystals of the Fe salt, on the contrary, the spin−flop field B_{SF}, which appears as a kink in the magnetization curve, shows pressure dependence (Figure 4a; 0.7 T at 1 bar, 1.2 T at 9.1 kbar). Figures 3c and 4b illustrate the hysteresis loops measured at $T = 2$ K for the Cr and Fe salts, respectively. As the pressure increases, the magnetization at $B = 0$ T, i.e., $M_r(2,p)$ of the Cr salt, decreases while that of the Fe salt increases. The coercive force of the Cr salt is 12 mT and has no significant pressure dependence. For the Fe salt, the coercive force cannot be

(30) Wada, M.; Takeda, K.; Ohtani, A.; Onodera, A.; Haseda, T. *J. Phys. Soc. Jpn.* **1983**, *52*, 3188−3198.

determined because a nonoriented sample was used for the measurement. Figure 4c presents the pressure dependence of the saturation field B_{SAT} of the Cr and Fe salts, estimated by extrapolating the magnetization curve to $M = 4$ and 6 μ_B for the Cr ($S = {}^3/_2$) and Fe ($S = {}^5/_2$) salts, respectively. As the pressure increases, B_{SAT} monotonically increases for both salts, showing the increase of the intermolecular AF interaction. However, their sensitivity to the pressure has a remarkable difference. For the Cr salt, B_{SAT} at 9.4 kbar is ca. 4 T larger than the value at the ambient pressure, whereas for the Fe salt, the increment of B_{SAT} is less than 1 T in the same pressure.

The temperature dependence of the cell parameters reveals that the thermal contraction of these salts is anisotropic. For both salts, the cell length c at $T = 18$ K is ca. 2% smaller than the value at $T = 293$ K, whereas the relative decrease in the cell lengths a and b is estimated at 1%. It should be noted that the cell angle β monotonically decreases as the temperature decreases, showing that the thermal contraction of the lattice has a significant contribution of the shear phonon mode. Because of this anisotropy, the thermal contraction of the intermolecular S···S distances, which is responsible for the intermolecular exchange interaction, is not uniform. Figures 5a and 4b show the temperature dependence of the intermolecular S···S distances of the Cr and Fe salts, respectively. For both salts, the temperature dependence of the S···S distance between anions (d−d; filled squares) is more significant than that of the donor−anion distance within a donor−anion alternating chain (π−d; open circles, open squares, and triangles) or the donor−donor distance of neighboring chains ($\pi-\pi$; filled circles). Indeed, the thermal contraction of the anion−anion distance is about doubled in comparison with that for the donor−donor distance for both salts.

Discussion

The magnetic properties for the Cr and Fe salts are similar to the fact that the application of the pressure increases the magnetic transition temperature T_c. Because T_c is directly correlated to the magnitude of the AF interactions, it is indicated that intermolecular AF interactions are increased with an increase in the pressure for both salts. Moreover, the increase of the saturation field B_{SAT} of both salts by applying pressure consistently shows the pressure-induced increases in the intermolecular AF interactions between the localized moments.

However, the detailed pressure effects on the magnetic behaviors are different between these two salts. The remanent magnetization $M_r(0,p)$ of the Cr salt shows significantly larger decreases than the Fe salt as the pressure enhances the AF magnetic interactions. As we have discussed in a previous paper,[12] the origin of the remanent magnetization is ascribed to be the spin canting due to the noncollinear alignment of the anions on the adjacent ferromagnetic chains. Because of this geometrical configuration, the presence of single-ion anisotropy and D−M interaction between the adjacent anions causes spin-canted alignment and thus nonvanishing total magnetic moments. The canting angle is roughly estimated at $\tan^{-1}|D/2J|$, where J is the AF exchange interaction between two neighboring spins and D is the antisymmetrical term from single-ion anisotropy and D−M interaction. Because single-ion anisotropy is determined by the geometry of the individual magnetic anions and thus is pressure-insensitive, the canting angle governed by single-ion anisotropy should give a negative pressure dependence. On the contrary, the magnitude of the D−M interaction D increases as the AF interaction J increases; hence, the canting angle governed by D−M interaction should have a small pressure dependence. For the Cr salt, the spin-canting angle defined as $\sin^{-1}[M_r(0,p)/2\ \mu_B]$, whose value is 2.9° at ambient pressure,[12] becomes reduced as a result of the stronger AF interaction in the higher pressure region, suggesting that the spin canting is governed by a competition between the AF interaction and single-ion anisotropy, which has a larger contribution than the D−M interaction. On the contrary, the spin-canting angle of the Fe salt $\{\sin^{-1}[M_r(0,p)/4\ \mu_B]\}$ has a smaller pressure dependence than the Cr salt, suggesting that single-ion anisotropy is less contributed and that the spin canting is determined by the D−M interaction. The difference of the contribution of single-ion anisotropy to the spin canting between these two salts is explained as follows. For the quartet ($S = {}^3/_2$) state of the $[Cr^{III}(isoq)_2(NCS)_4]^-$ complex, the contribution of excited state $^4T_{2g}$ $[(t_{2g})^2(e_g)^1]$ to ground state $^4A_{2g}$ $[(t_{2g})^3]$ gives a negative zero-field-splitting constant $D < 0$ for the prolate ligand field, if the covalent character of the metal−ligand bonds is taken into account.[31] On the contrary, for the sextet ($S = {}^5/_2$) state of $[Fe^{III}(isoq)_2(NCS)_4]^-$, there is no contribution of the spin excited state with the same spin multiplicity to the totally symmetrical ground state $^6A_{1g}$ $[(t_{2g})^3(e_g)^2]$. The zero-field-splitting constant D of the Fe complex is, therefore, smaller than the Cr complex with similar coordination distortion.

Because the analysis of the magnetic structure is difficult for the randomly oriented crystals of the Fe salt because of the lack of information about magnetic anisotropy, hereafter we focus on the Cr salt for the quantitative analysis of the pressure dependence of its magnetic structure based on the mean-field approximation. Figure 1b shows the spin structure model used on the present analysis, in which a unit cell of four sublattices contains two localized π spins π_i ($i = 1, 2$) and two d spins d_i ($i = 1, 2$) illustrated with short and long arrows, respectively. There are three types of exchange interactions, namely, $J_{\pi\pi}$ representing the interaction between the donors (black dotted line in Figure 1b), $J_{\pi d}$ representing the donor−anion interaction (black solid lines), and J_{dd} representing the anion−anion interaction (gray solid line). The spin Hamiltonian of this material is expressed as

$$H = H_{ex} + H_{anis} + H_{Zeeman} \quad (2)$$

where H_{ex}, H_{anis}, and H_{Zeeman} represent the exchange interaction, magnetic anisotropy, and Zeeman energy terms, respectively. The exchange term H_{ex} is expressed as

(31) Neese, F.; Solomon, E. I. In *Magnetism: Molecules to Materials IV*; Miller, J. S., Drillon, M., Eds.; Wiley-VCH: Weinheim, Germany, 2003; Chapter 9.

$$H_{ex} = -\sum_{\langle i,j \rangle} 2J_{\pi\pi}\mathbf{s}_i\cdot\mathbf{s}_j - \sum_{\langle i,k \rangle} 2J_{\pi d}\mathbf{s}_i\cdot\mathbf{S}_k - \sum_{\langle k,l \rangle} 2J_{dd}\mathbf{S}_k\cdot\mathbf{S}_l \quad (3)$$

where $\mathbf{s}_i$ and $\mathbf{S}_k$ represent π and d spins, respectively. We take account of single-ion anisotropy for the anion complex because the CrN_6 coordination octahedron is elongated to the direction of the isoquinoline ligand.[12] The anisotropic term H_{anis} is

$$H_{anis} = \sum_k D(S_k^z)^2 \quad (4)$$

where S_k^z and D represent the molecular axis (isoq−Cr−isoq) component of the spin $\mathbf{S}_k$ and the zero-field-splitting constant of the Cr complex, respectively. Finally, the Zeeman term H_{Zeeman} is described as

$$H_{Zeeman} = \sum_q g\mu_B\mathbf{s}_q\cdot\mathbf{B} + \sum_r g\mu_B\mathbf{S}_r\cdot\mathbf{B} \quad (5)$$

where g, μ_B, and $\mathbf{B}$ represent the g value, Bohr magneton, and external field, respectively. Here we assume for simplicity $g = 2$ and treat spin operators $\mathbf{s}_i$ and $\mathbf{S}_k$ as classical continuous vectors. The coordination numbers z are 2 for all three terms in H_{ex}, as illustrated in Figure 1b. Under these approximations, the total energy E calculated from the Hamiltonian (2) under the magnetic field along the b axis is expressed as

$$\begin{aligned} E = \frac{N}{2}[&-J_\pi\pi\cos(\varphi_{\pi_1} - \varphi_{\pi_2}) - 3J_{\pi d}\{\cos(\varphi_{d_1} - \varphi_{\pi_1})] + \\ &\cos(\varphi_{d_2} - \varphi_{\pi_2})\} - 9J_{dd}\cos(\varphi_{d_1} - \varphi_{d_2}) + \\ &\frac{9}{4}D\{\cos^2(\varphi_{d_1} - \theta_{d_1}) + \cos^2(\varphi_{d_2} - \theta_{d_2})\} + \\ &\mu_B B\{(\sin\varphi_{\pi_1} + \sin\varphi_{\pi_2}) + 3(\sin\varphi_{d_1} + \sin\varphi_{d_2})] \quad (6) \end{aligned}$$

where N, φ_i ($i = \pi_1, \pi_2, d_1, d_2$), and θ_j ($j = d_1, d_2$) represent Avogadro's number, the canting angles of each spin from the ac plane, and the canting angle of the molecular axis (isoq−M−isoq axis) from the ac plane, respectively, as illustrated in Figure 1c. Because $\theta_{d_1} = \pi - \theta_{d_2}$ ($\equiv\theta_d = 34.5°$) and assuming that $\varphi_{\pi_1} = \pi - \varphi_{\pi_2}$ ($\equiv\varphi_\pi$) and $\varphi_{d_1} = \pi - \varphi_{d_2}$ ($\equiv\varphi_d$), eq 6 is simplified as

$$\begin{aligned} E = \frac{N}{2}\Big[&J_{\pi\pi}\cos 2\varphi_\pi - 6J_{\pi d}\cos(\varphi_d - \varphi_\pi) + 9J_{dd}\cos 2\varphi_d + \\ &\frac{9}{2}D\cos^2(\varphi_d - \theta_d) + 2\mu_B B(\sin\varphi_\pi + 3\sin\varphi_d)\Big] \quad (7) \end{aligned}$$

The most stable magnetic structure is obtained by minimizing the energy E with respect to φ_π and φ_d, and the magnetization along the b axis $M = -\partial E/\partial B = -N\mu_B(\sin\varphi_\pi + 3\sin\varphi_d)$ can be expressed as a function of the field B. The magnetization curves at various pressures (Figure 3a) are fitted with those calculated with the least-squares method, using the exchange interactions J_i ($i = \pi\pi$, πd, dd) and the zero-field-splitting constant D as fitting parameters.

The present model satisfactorily explains the experimental data as evidenced in the top panel of Figure 6a for two representative data sets $p = 1$ bar and 8.7 kbar. The bottom panel of Figure 6a gives the field dependence of the canting angles for the π spins φ_π and d spins φ_d for these two pressures. The magnetization is mainly governed by the spin canting of the d-electron spins that is more sensitive to the applied field, which is the consequence of the larger magnitude of the d-electron spins and the presence of the single-ion anisotropy term of the complex anions. The fitting gives the values of the parameters at ambient pressure: $J_{\pi\pi} = -13$ K, $J_{\pi d} = -3.0$ K, $J_{dd} = -0.35$ K, and $D = -0.22$ K. Here we compare the exchange interactions experimentally obtained at the ambient pressure with the theoretical calculation results based on the extended Hückel method ($J_{\pi\pi} =$

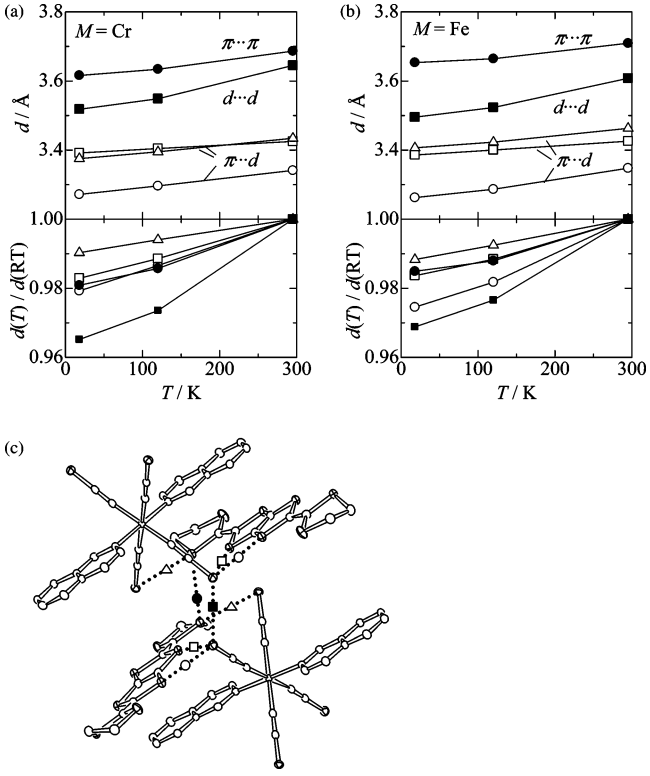

Figure 5. Temperature dependence of the intermolecular S···S distances of (BDH-TTP)[M(isoq)$_2$(NCS)$_4$]: (a) M = Cr; (b) M = Fe. Lower panels are S···S distances normalized with a value at 295 K. Open circles, squares, and triangles filled circles and squares in both panels designate the S···S contacts in Figure 4c, indicated as dotted lines with the same symbols. Solid lines are guides for the eyes.

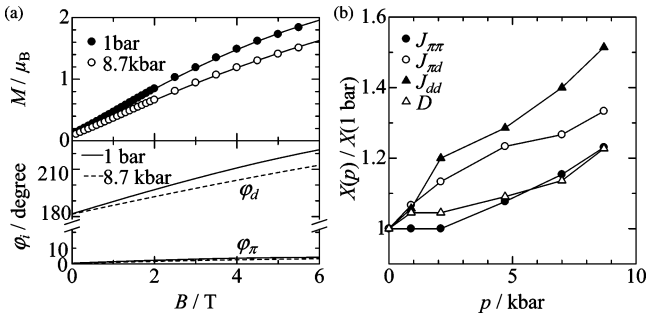

Figure 6. (a) Top panel: magnetization curves of the Cr salt measured at $T = 2$ K with B parallel to b under ambient pressure (filled circles) and $p = 8.7$ kbar (open circles). Solid lines are magnetization curves obtained from the theoretical model described in the text. Bottom panel: pressure dependence of the canting angles of π spins φ_π and d spins φ_d for ambient pressure (solid lines) and $p = 8.7$ kbar (dashed lines). (b) Pressure dependence of the exchange interactions J_i ($i = \pi\pi$, πd, dd) and the zero-field-splitting parameter, normalized by the values at the ambient pressure. Solid lines are guides for the eyes.

Table 2. Pressure Dependence of the Exchange Interactions J_i ($i = \pi\pi$, πd, dd), the Zero-Field-Splitting Constant D, the Calculated Magnetic Transition Temperature T_c, and the Calculated Weiss Temperature Θ for (BDH-TTP)[Cr(isoq)$_2$(NCS)$_4$]

p/kbar	0[a]	0.9	2.1	4.7	7.0	8.7
$J_{\pi\pi}$/K	−13	−13	−13	−14	−15	−16
$J_{\pi d}$/K	−3.0	−3.2	−3.4	−3.7	−3.8	−4.0
J_{dd}/K	−0.35	−0.37	−0.42	−0.45	−0.49	−0.53
D/K	−0.22	−0.23	−0.23	−0.24	−0.25	−0.26
T_c/K	8.0	8.1	8.5	9.1	9.8	10.1
Θ/K	−1.7	−1.8	−1.9	−2.1	−2.2	−2.3

[a] Ambient pressure (1 bar).

−22.8 K, $J_{\pi d} = -9.63$ K, and $J_{dd} = -2.24$ K).[32] The magnitude of the exchange interaction obtained by fitting is one-sixth to half of the estimation of the extended Hückel calculation. Considering the crudeness of the extended Hückel calculation, this accordance should be regarded as a conceivable one. The negative value of D suggests that the localized spins on the Cr complex orient along the Cr−isoq molecular axis, supporting the previous discussion on the spin structure in the ordered phase.[12]

Table 2 summarizes the exchange interactions and zero-field-splitting constants for each pressure obtained by the mean-field fittings. Figure 6b gives the pressure dependence of the exchange interactions J_i ($i = \pi\pi$, πd, dd) and the zero-field-splitting constant D, normalized by the values at ambient pressure. As the pressure increases, the absolute values of these parameters increase, reflecting the increase of the intermolecular contacts. The pressure dependence of J_{dd} is more significant than those of $J_{\pi\pi}$ and $J_{\pi d}$, which can be rationalized as follows. According to the Grüneisen relation $\alpha = \gamma\kappa C_V/V$ (α = thermal expansion coefficient, γ = Grüneisen constant, κ = isothermal compressibility, and C_V = constant-volume heat capacity), the pressure dependence of the crystal structure is connected with the temperature dependence. Namely, the *pressure* dependence of J (Figure 6b) is related to the *temperature* dependence of the intermolecular S···S distance (Figure 5a) because the interchain donor−anion S···S distance (∼3.4 Å) at 295 K is significantly smaller than twice that of the van der Waals radius of a S atom ($2 \times 1.75 = 3.7$ Å), in contrast to the interchain donor−donor and anion−anion distances. In other words, the donor−anion intermolecular contacts are the stiffest among the intermolecular contacts. Therefore, the intermolecular contacts along the donor−anion alternating chains are less sensitive to the temperature, giving the smaller pressure dependence of $J_{\pi d}$. On the other hand, because the interchain S···S distances (∼3.6 Å) are moderate ones, the interchain contacts have a stronger temperature dependence than the intrachain contacts, corresponding to the pressure sensitivity of J_{dd}. As for $J_{\pi\pi}$, the present analysis shows that this interaction little affects the magnetization curves because of the small canting angle of the π electron. Accordingly, the estimate of $J_{\pi\pi}$ may contain a larger error in the least-squares fittings, and thus it is difficult to compare its pressure dependence with the others. The zero-field-splitting parameter D also shows pressure dependence, although the crystal structure analysis gives no significant temperature dependence of the Cr−N bond lengths within experimental errors. The reason for this difference may be related to the molecular geometry change characteristic of the compression. This possibility will be clarified by the crystal structure analysis under pressure.

Finally, we comment on the pressure dependence of the magnetic transition temperature. Under the molecular-field approximation, the transition temperature T_c and the Weiss temperature are given by

$$T_c = \frac{1}{4}[-(J_{\pi\pi} + 5J_{dd}) + \sqrt{(J_{\pi\pi} - 5J_{dd})^2 + 20J_{\pi d}{}^2}] \quad (8)$$

and

$$\Theta = \frac{J_{\pi\pi} + 10J_{\pi d} + 25J_{dd}}{12} \quad (9)$$

respectively.[32] From the exchange interactions J_i ($i = \pi\pi$, πd, and dd) obtained by the least-squares fitting, T_c and Θ are calculated as summarized in Table 2. The transition temperature at ambient pressure $T_c = 8.0$ K is in good agreement with the experimental result $T_c = 7.6$ K.[12] Of course, this agreement must be just a chance because the present approximations are too crude to represent the spin state of this material correctly. There is no consideration of the contribution of the magnetic anisotropy and spin fluctuations, the latter of which are critical in the vicinity of T_c. In fact, the pressure dependence of T_c is about half of the experimental results, and the Weiss temperature $\Theta = -1.73$ K at ambient pressure is too much smaller than the experimental value $\Theta = -40$ K. The latter discrepancy especially shows the insufficiency of the mean-field approximation, which is mainly caused by neglecting the short-range ordering effect in the present analysis. Indeed, this effect is experimentally suggested by the single-crystal EPR measurement of the Cr salt.[13] As the temperature decreases, the g value of a single Lorentzian signal decreases for B parallel to the a and b directions and increases for B parallel to the c direction below $T \sim 100$ K, which is a sufficiently higher temperature than the magnetic ordering temperature. These anisotropic g shifts are explained as a result of short-range order of the spins if a spin Hamiltonian contains anisotropic terms.[33]

Conclusion

The magnetic properties of bulk spin-canting weak-ferromagnetic ferrimagnets (BDH-TTP)[M(isoq)$_2$(NCS)$_4$] (M = Cr, Fe) with T_c of 7.6 K under high pressure and the structural change by the decreasing temperature were investigated. It is observed that the application of pressure enhanced T_c for both M = Cr and Fe up to 16.6 and 11.6 K at 9 kbar, respectively. The pressure dependence of the remanent magnetization suggests that, for the Cr salt, single-ion anisotropy mainly governs the spin canting, whereas the D−M interaction does so for the Fe salt. The analysis of the

(32) Katsuhara, M.; Mori, T. *J. Phys. Soc. Jpn.* **2003**, *73*, 3335−3340.

(33) Nagata, K.; Tazuke, Y. *J. Phys. Soc. Jpn.* **1972**, *32*, 337−345.

magnetization curves for the Cr salt based on the molecular-field approximation reveals that the large pressure dependence of the magnetic transition temperature is due to the pressure dependence of the intermolecular exchange interaction, especially J_{dd}, between the transition-metal anions. This result is also supported by the fact that the S···S contacts between the anions shows the most significant temperature dependence. Moreover, the spin structure of these molecular magnets is determined by the competition between the exchange interaction and magnetic anisotropy (Cr, mainly single-ion anisotropy; Fe, mainly the D−M interaction) of the transition-metal anions. The application of the external pressure increases the intermolecular exchange interaction, which affects the competition to modify the spin structure of these salts.

Acknowledgment. The authors express their thanks to Dr. Loïc Toupet (GMCM, Université de Rennes 1) for X-ray diffraction measurements at He temperature. The present work was financially supported by the Japan−France Research Cooperative program, CNRS−JSPS PICS program No. 1433, and Grants-in-Aid (Grants 14540530 and 15073211) from the Ministry of Education, Science, Sports, and Culture, Japan.

Supporting Information Available: Full atomic coordinates, bond lengths, and bond angles (CIF). This material is available free of charge via the Internet at http://pubs.acs.org.

IC0518778